

Active Sampling for Accelerated MRI with Low-Rank Tensors

Zichang He^{*}, Bo Zhao[†], and Zheng Zhang^{*}

^{*} Department of Electrical and Computer Engineering, University of California, Santa Barbara

[†]Oden Institute for Computational Engineering and Sciences and

Department of Biomedical Engineering, University of Texas at Austin

Emails: zichanghe@ucsb.edu, bozhao@utexas.edu, zhengzhang@ece.ucsb.edu

Abstract—Magnetic resonance imaging (MRI) is a powerful imaging modality that revolutionizes medicine and biology. The imaging speed of high-dimensional MRI is often limited, which constrains its practical utility. Recently, low-rank tensor models have been exploited to enable fast MR imaging with sparse sampling. Most existing methods use some pre-defined sampling design, and active sensing has not been explored for low-rank tensor imaging. In this paper, we introduce an active low-rank tensor model for fast MR imaging. We propose an active sampling method based on a Query-by-Committee model, making use of the benefits of low-rank tensor structure. Numerical experiments on a 3-D MRI data set demonstrate the effectiveness of the proposed method.

I. INTRODUCTION

Magnetic resonance imaging is a major medical imaging modality, which is widely used in clinical diagnosis and neuroscience. Due to the limited imaging speed, it is often highly desirable to speed up its imaging process. A lot of image models have been proposed to accelerate MR imaging, including sparsity-constrained [1], low-rank-constrained [2–4], data-driven, learning-based approaches, etc [5]. Most of these methods recover MRI data with matrix computational techniques. They either focus on 2-D MRI problems [6] or reshape the high-dimensional MRI data into a matrix and then solve the problem using matrix-based techniques [7].

As a multi-dimensional generalization of matrix computation, tensor computation has been recently employed in MRI due to its capability of handling high-dimensional data [8–10]. In many applications, MRI data sets naturally have a higher physical dimension. In these cases, tensors often better capture the hidden high-dimensional data pattern, achieving better reconstruction performance [11, 12].

The quality and efficiency of an MRI reconstruction also highly depend on the sampling method. Practical samples are measured in the spatial frequency domain of an MR image, often known as k -space. Some adaptive sampling techniques have been proposed for matrix-format MR imaging based on compressive sensing or low-rank models [13, 14]. The experimental design methodologies include the Bayesian model [15], learning-based framework [16–18], self-supervised framework [19], and so forth. Adaptive samplings may also be considered for streaming data [20].

However, active sampling has not been explored for fast MR imaging with low-rank tensor models. Beyond the application

of MR imaging, there are also limited works of adaptive sampling for tensor-structured data. Existing works mainly rely on the matrix coherence property [21–23]. They need to reshape the tensor to a matrix or can only apply on a 3-D tensor. Additionally, the practical MRI sampling is usually subject to some pattern constraints, like a Cartesian line sampling. Few papers have considered the pattern constraints caused by the practical MRI sampling. Therefore, designing an active sampling method for tensor-structured data under certain pattern constraints is an important and open problem.

Paper contributions. This paper presents an active sampling method for accelerating high-dimensional MR Imaging with low-rank tensors. Our specific contributions include:

- Novel active sampling methods for low-rank tensor-structured MRI data. A Query-by-Committee method is used to search for the most informative sample adaptively. Making use of the special tensor structure, the approximations towards the unfolding matrices naturally forms a committee. The sample quality is measured by the predictive variance, averaged leverage scores, or their combinations.
- Extending the sampling method to handle some pattern constraints in MR imaging. Our proposed sampling method can be applied broadly beyond MRI reconstruction.
- Numerical validation on an MRI example with Cartesian sampling. Numerical results show that the proposed methods outperform the existing tensor sampling methods.

II. BACKGROUND

A. Notation

Throughout this paper, a scalar is represented by a lowercase letter, *e.g.*, x ; a vector or matrix is represented by a boldface lowercase or capital letter respectively, *e.g.*, \mathbf{x} and \mathbf{X} . A tensor, which describes a multidimensional data array, is represented by an Euler script calligraphic letter. For instance, a n -dimensional tensor is denoted as $\mathcal{X} \in \mathbb{R}^{I_1 \times I_2 \times \dots \times I_n}$, where I_i is the mode size of the i -th mode (or dimension). An element indexed by (i_1, i_2, \dots, i_n) in tensor \mathcal{X} is denoted as $x_{i_1 i_2 \dots i_n}$. A tensor Frobenius norm is defined as $\|\mathcal{X}\|_F := \sqrt{\sum_{i_1, i_2, \dots, i_n} (x_{i_1 i_2 \dots i_n})^2}$. A tensor $\mathcal{X} \in \mathbb{R}^{I_1 \times I_2 \times \dots \times I_n}$ can be unfolded into a matrix along the k -th mode/dimension, denoted as $\text{Unfold}_k(\mathcal{X}) := \mathbf{X}_{(k)} \in \mathbb{R}^{I_k \times I_1 \dots I_{k-1} I_{k+1} \dots I_n}$. Conversely,

folding the k -mode matricization back to the original tensor is denoted as $\text{Fold}_k(\mathbf{X}_{(k)}) := \mathcal{X}$.

B. Tensor-Format MRI Reconstruction

In tensor completion, one aims to predict a whole tensor given only partial elements of the tensor, which is similar with matrix completion. In matrix cases, one often uses the nuclear norm $\|\cdot\|_*$ (sum of singular values) as a surrogate of a matrix rank, and seeks for a matrix with the minimal nuclear norm. Exactly computing the tensor rank is NP-hard [24]. A popular heuristic surrogate of tensor (Tucker) rank is the generalization of matrix nuclear norms [25]:

$$\|\mathcal{X}\|_* = \sum_{i=1}^n \alpha_i \|\mathbf{X}_{(i)}\|_*, \quad (1)$$

where $\{\alpha_i\}_{i=1}^n$ are the weights, satisfying $\alpha_i > 0$ and $\sum_{i=1}^n \alpha_i = 1$. Then the tensor completion problem can be formulated as minimizing Eq. (1) given existing observations.

The above mode- n matricization $\{\mathbf{X}_{(i)}\}_{i=1}^n$ represents the same set of data and thus are coupled to each other, which makes it hard to solve. Therefore, we replace them with n additional matrices $\{\mathbf{X}_i\}_{i=1}^n$ and introduce an additional tensor \mathcal{M} . The optimization problem can be reformulated as:

$$\begin{aligned} \min_{\{\mathbf{X}_i\}_{i=1}^n, \mathcal{M}} \quad & \sum_{i=1}^n \alpha_i \|\mathbf{X}_i\|_* \\ \text{s.t.} \quad & \mathbf{X}_i = \mathbf{M}_{(i)}, \quad i = 1, 2, \dots, n \\ & \mathcal{M}_\Omega = \mathcal{T}_\Omega. \end{aligned} \quad (2)$$

where \mathcal{M} is a tensor in the k -space; $\mathbf{M}_{(i)}$ is the i -th mode matricization of \mathcal{M} ; \mathcal{T} is the fully sampled k -space tensor and Ω is its observation set. Essentially, we can either model the low-rankness of the k -space or the image space data. We choose the former one since it enables the design of our active sampling methods in Section III. If the MRI data is known to hold some additional structure, we can further modify the imaging model by adding a regularization term, like the low rank plus sparsity model [26].

Eq. (2) can be efficiently solved via some alternating solvers, like block coordinate descent and alternating direction method of multipliers (ADMM) [25]. Our proposed active sampling strategies will exploit these additional mode approximations $\{\mathbf{X}_i\}_{i=1}^n$ to acquire new k -space samples.

III. ACTIVE TENSOR SAMPLING METHOD

The complete flowchart of our MRI reconstruction framework is illustrated in Fig. 1. In order to design an active sampling method for MRI reconstruction, two questions need to be answered: (1) How can we pick informative samples? (2) How can we guarantee that the new samples obey the patterns of MRI scans? We will provide the details in this section.

A. Query-by-Committee-based Active Sampling

We are inspired by a classical active learning approach called Query-by-Committee [27]. The key idea is to employ a committee of different models to predict the response values at

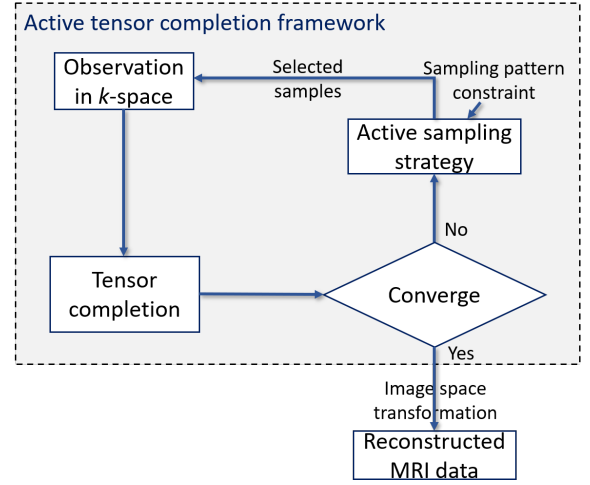


Fig. 1. Flowchart of the MRI reconstruction framework.

some candidate samples respectively. With such a committee, we can measure the quality of a candidate sample and pick the optimal one. The two key components of the Query-by-Committee approach are

- **A committee of models.** The different tensor mode unfolding matrices obtained from solving Eq. (2) can naturally form a model committee required by our active sampling method. This model committee enables us to define an element-wise utility measure, denoted as $u(\xi)$, where ξ is an element in the tensor.
- **Measure of sample quality.** After constructing a committee of model, we can define a measure of sample quality u . The sample with the largest u will be selected and added into the observation set: $\Omega \leftarrow \Omega \cup \arg\max_{\xi} u(\xi)$. We consider the predictive variance and leverage score as well as their combinations as our measure of sample quality, as detailed in next sub-section.

B. Measure of Sample Quality

Predictive variance. The first choice is the predicted variance from different tensor modes. Based on the solved \mathbf{X}_i , if we unfold it and enforcing its consistency with the observed data, we can obtain mode- i low-rank approximation to \mathcal{M} :

$$\tilde{\mathcal{M}}_i := \text{Fold}_i(\mathbf{X}_i), \quad \tilde{\mathcal{M}}_i(\Omega) \leftarrow \mathcal{T}(\Omega). \quad (3)$$

We define the difference tensor of each approximation $\Delta\mathcal{M}_i$ and the predictive variance tensor \mathcal{V} as:

$$\Delta\mathcal{M}_i := \tilde{\mathcal{M}}_i - \mathbb{E}[\tilde{\mathcal{M}}], \quad \mathcal{V} := \sum_{i=1}^n w_i (\Delta\mathcal{M}_i \circ \Delta\mathcal{M}_i) \quad (4)$$

where \circ denotes a Hadamard (element-wise) product, and w_i is the weight associated with mode- i approximation $\tilde{\mathcal{M}}_i$. The value of w_i depends on the solver to Eq. (2). In our implementation, we adopt ADMM solver and have $\{w_i\}_{i=1}^n = \frac{1}{n}$. Here, $\mathbb{E}[\tilde{\mathcal{M}}] := \sum_{i=1}^n w_i \tilde{\mathcal{M}}_i$ is the expectation of all n mode

approximations. Among the n mode approximation tensors $\{\tilde{\mathcal{M}}_i\}_{i=1}^n$, some of the estimated entries are the same or similar with the true data (with small variance), while some other estimated entries are very different (with large variance). Therefore, we can treat \mathcal{V} as a measure of disagreement. The following lemma describes the relation between the approximation error among different modes.

Lemma 1. *Let μ be the sum of all elements of the predictive variance tensor $\mu := \|\text{vec}(\mathcal{V})\|_1 = \sum_{i=1}^n w_i \|\Delta \mathcal{M}_i\|_F^2$. Denote*

μ_i be the mode- i approximation error: $\mu_i = \|\mathcal{M} - \tilde{\mathcal{M}}_i\|_F^2$, and μ_{tot} be the reconstruction error of the whole data set: $\mu_{\text{tot}} = \|\mathcal{M} - \mathbb{E}[\tilde{\mathcal{M}}]\|_F^2$, then we have

$$\mu_{\text{tot}} = \sum_{i=1}^n w_i \mu_i - \mu. \quad (5)$$

The approximation results of different modes gradually converge to the same one as more samples are observed. When the tensor is fully sampled, both μ and μ_{tot} approach zero. Heuristically, μ_{tot} decreases quickly when a sample with the highest predictive variance is selected.

Leverage score. Our second quality measurement u is the leverage score. It comes from the incoherence property of a matrix [28, 29]: a low-rank matrix can be recovered via nuclear norm minimization if it satisfies the incoherent property. Given the singular value decomposition (SVD) of a rank- r matrix $\mathbf{A} = \mathbf{U}\mathbf{\Sigma}\mathbf{V}^H \in \mathbb{C}^{n_1 \times n_2}$, the left and right leverage scores of a matrix are defined as:

$$\begin{aligned} \mathbf{l}(i) &:= \frac{n_1}{r} \|\mathbf{U}^T \mathbf{e}_i\|_2^2, \quad i = 1, 2, \dots, n_1, \\ \mathbf{r}(j) &:= \frac{n_2}{r} \|\mathbf{V}^T \mathbf{e}_j\|_2^2, \quad j = 1, 2, \dots, n_2. \end{aligned} \quad (6)$$

A leverage score measures the coherence of a row/column with a coordinate direction. Generally, the rows/columns with larger left/right scores are more informative. For the mode- k unfolded matrix of a tensor, we can perform SVD and calculate its left and right leverage scores as \mathbf{l}_k and \mathbf{r}_k respectively, then the element-level leverage score of a sample (i, j) in mode k is defined as:

$$\ell_k(i, j) := \mathbf{l}_k(i) \times \mathbf{r}_k(j), \quad k = 1, 2, \dots, n. \quad (7)$$

In a tensor structure, we can average the element-level leverage scores over modes and treat it as the utility measurement:

$$\ell_{i_1, \dots, i_n} := \sum_{i=1}^n w_i \text{Fold}_i(\ell_i). \quad (8)$$

Based on the above two measurements, we propose four greedy methods for our active tensor sampling as follows:

- **Method 1 (Var):** We take the utility measurement u as the variance among different modes [Eq. (4)].
- **Method 2 (Lev):** We take the utility measurement u as the averaged leverage scores [Eq. (8)].
- **Method 3 / 4 (Var + Lev/ Var \times Lev):** We take the utility measurement u as the sum/ Hadamard product of

the normalized variance [Eq. (4)] and the leverage scores [Eq. (8)].

C. Sampling under Pattern Constraint

Now we show how to pick the samples subject to a certain pattern constraint. Suppose the unobserved k -space data is partitioned into K patterns $\{\Pi_i\}_{i=1}^K$. For example, in a Cartesian sampling, the pattern Π_i is a rectilinear sampling, i.e. a full column or row in a k -space matrix (k_x - k_y). We are required to sample all samples of a certain pattern Π_i rather than just one element.

Since our utility measurements are calculated element-wisely in the Query-by-Committee, they can be easily applied to any sampling pattern by summing the utility measurement over all elements included in the pattern. Consequently, we have a pattern-wise measurement:

$$u(\Pi_i) = \sum_{\xi \in \Pi_i} u(\xi), \quad i = 1, 2, \dots, K. \quad (9)$$

As a result, the observation set can be updated as $\Omega \leftarrow \Omega \cup \text{argmax}_{\Pi_i} u(\Pi_i)$. Without any pattern constraints, Eq. (9) will degenerate to an element-wise measurement. In practical implementations, the active learning algorithm can be easily extended to a batch version. We can stop the algorithm when the algorithm runs out of a sampling budget.

IV. NUMERICAL RESULTS

In this section, we validate our active sampling methods on a low-rank tensor-format MRI data set. Our codes are implemented in MATLAB and run on a computer with 2.3GHz CPU and 16GB memory.

Data set. We use a 3D-spatial MRI data¹ to demonstrate the proposed active tensor completion model. This data set has some cardiac MR images acquired from 33 subjects. The sequence of each subject consists of 20 time frames and 8-15 slices along the third spatial axis [30]. We select one frame of one subject with size $256 \times 256 \times 10$ for validation here.

Sampling Patterns. In each spatial slice, we initialize the sampling as a fully Cartesian sampled central region plus randomly Cartesian sampled non-central regions. In this case, the newly added samples should be a fiber in the k -space, which is obtained via fixing all but one index of the tensor.

Evaluation metrics. Our methods sample and predict k -space data, and the final reconstruction needs to be visualized in the image space. Therefore, we choose the evaluation metrics from both spaces. In the k -space, the accuracy is measured by the relative mean square error evaluated over the fully-sampled k -space data, denoted as k -test. In the image space, we use the signal to error ratio (SER) and peak signal to noise ratio (PSNR) as our metrics:

$$\text{SER} := -10 \log_{10} \frac{\|\mathcal{I}_{\text{res}} - \mathcal{I}_{\text{full}}\|_F}{\|\mathcal{I}_{\text{full}}\|_F} \quad (10)$$

$$\text{PSNR} := 20 \log_{10} \frac{\max(\mathcal{I}_{\text{res}})}{\sqrt{\text{MSE}(\mathcal{I})}}. \quad (11)$$

¹Available at <http://www.cse.yorku.ca/~mridataset/>

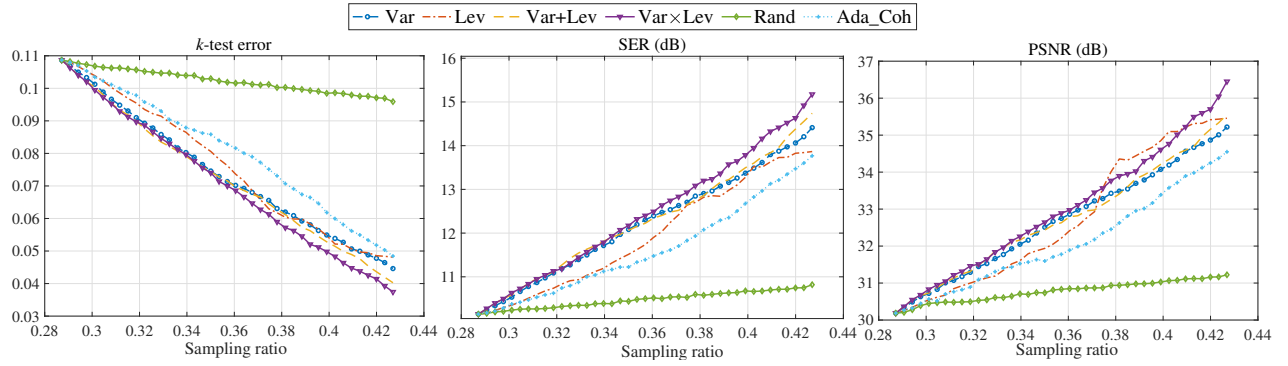


Fig. 2. Reconstruction results of different adaptive sampling methods. The proposed methods all outperform the existing Ada_Coh and random methods. Method 4 (Var \times Lev) is the most suitable one in this example.

TABLE I
EVALUATIONS ON THE WHOLE DATA SET.

	Initial	Ada_Coh	Proposed (Method 4)
SER (dB)	10.15	13.77	15.17
PSNR (dB)	30.19	34.55	36.45

Here \mathcal{I}_{res} and $\mathcal{I}_{\text{full}}$ denote the reconstructed and true image space data, and $\text{MSE}(\mathcal{I})$ is their mean square error.

Baselines for Comparisons. We perform the experiments via adopting the proposed active learning methods, a matrix-coherence-based adaptive tensor sampling method (denoted as Ada_Coh) [21], and a random sampling method.

Results Summary. In this example, the k -space data is scanned continuously as a fiber in the Cartesian coordinate. The initial data is generated with a sampling ratio of 28.37%, including a 10.55% fully sampled center. In active sampling, each sampling batch includes 10 fibers, and we select a total of 40 batches in sequentially. Fig. 2 plots the k -test, SER and PSNR as the sampling ratios increase. All proposed active sampling methods can significantly improve the evaluation metrics and outperform Ada_Coh. Note that in [21], the sampling is driven by the coherence of one mode matricization of a tensor. Our Method 2 (Lev) can be seen as its generalization via taking consideration of the connections among different modes. Fig. 3 shows the reconstructed one frame of the MRI data and the evaluations of the whole data set are shown in Table I. The proposed sampling method is shown to have the least reconstruction error.

V. CONCLUSION

In this paper, we have presented a tensor-format active sampling model for reconstructing high-dimensional low-rank MR images. The proposed k -space active sampling approach is based on the Query-by-Committee method. It can easily handle various pattern constraints in practical MRI scans. Numerical results have shown that the proposed active sampling methods outperform the existing matrix-coherence-based adaptive sampling method. In the future, we will develop the theoretical

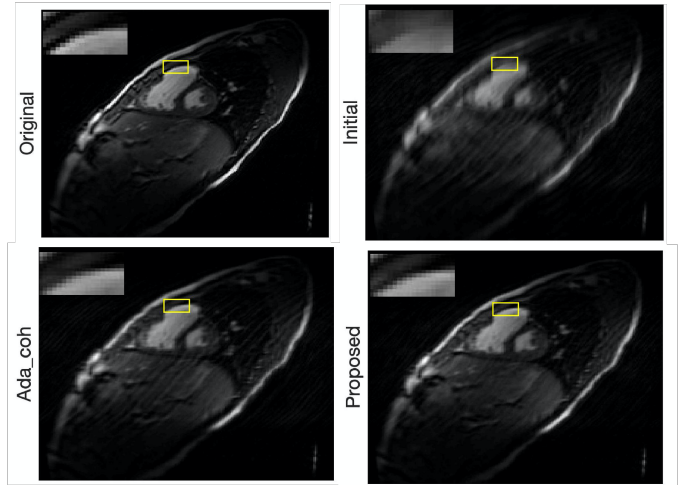


Fig. 3. Reconstructed one frame of the data.

analysis of the sampling model and verify it on more realistic MRI data.

REFERENCES

- [1] M. Lustig, D. Donoho, and J. M. Pauly, "Sparse MRI: The application of compressed sensing for rapid MR imaging," *Magn. Reson. Med.*, vol. 58, no. 6, pp. 1182–1195, 2007.
- [2] Z.-P. Liang, "Spatiotemporal imaging with partially separable functions," in *Intl. Symp. Biomedical Imaging: From Nano to Macro*, 2007, pp. 988–991.
- [3] S. G. Lingala, Y. Hu, E. DiBella, and M. Jacob, "Accelerated dynamic MRI exploiting sparsity and low-rank structure: kt SLR," *IEEE Trans. Med. Imag.*, vol. 30, no. 5, pp. 1042–1054, 2011.
- [4] B. Zhao, J. P. Haldar, A. G. Christodoulou, and Z.-P. Liang, "Image reconstruction from highly undersampled (k, t)-space data with joint partial separability and sparsity constraints," *IEEE Trans. Med. Imag.*, vol. 31, no. 9, pp. 1809–1820, 2012.
- [5] S. Ravishanker, J. C. Ye, and J. A. Fessler, "Image reconstruction: From sparsity to data-adaptive methods and machine learning," *Proc. of the IEEE*, vol. 108, no. 1, pp. 86–109, 2019.
- [6] J. Huang, S. Zhang, and D. Metaxas, "Efficient mr image reconstruction for compressed mr imaging," *Med. Image Anal.*, vol. 15, no. 5, pp. 670–679, 2011.

- [7] R. Otazo, E. Candes, and D. K. Sodickson, "Low-rank plus sparse matrix decomposition for accelerated dynamic MRI with separation of background and dynamic components," *Magn. Reson. Med.*, vol. 73, no. 3, pp. 1125–1136, 2015.
- [8] Y. Yu, J. Jin, F. Liu, and S. Crozier, "Multidimensional compressed sensing MRI using tensor decomposition-based sparsifying transform," *PLoS one*, vol. 9, no. 6, p. e98441, 2014.
- [9] F. Liu, D. Li, X. Jin, W. Qiu, Q. Xia, and B. Sun, "Dynamic cardiac MRI reconstruction using motion aligned locally low rank tensor (MALLRT)," *Magn. Reson. Imaging*, vol. 66, pp. 104–115, 2020.
- [10] J. D. Trzasko and A. Manduca, "A unified tensor regression framework for calibrationless dynamic, multi-channel mri reconstruction," in *Proc. ISMRM*, vol. 603, 2013, p. 21.
- [11] J. He, Q. Liu, A. G. Christodoulou, C. Ma, F. Lam, and Z.-P. Liang, "Accelerated high-dimensional mr imaging with sparse sampling using low-rank tensors," *IEEE Trans. Med. Imag.*, vol. 35, no. 9, pp. 2119–2129, 2016.
- [12] C. I. Kanatsoulis, X. Fu, N. D. Sidiropoulos, and M. Akçakaya, "Tensor completion from regular sub-nyquist samples," *IEEE Trans. Signal Process.*, vol. 68, pp. 1–16, 2019.
- [13] J. P. Haldar and D. Kim, "OEDIPUS: an experiment design framework for sparsity-constrained MRI," *IEEE Trans. Med. Imag.*, vol. 38, no. 7, pp. 1545–1558, July 2019.
- [14] E. Levine and B. Hargreaves, "On-the-fly adaptive k -space sampling for linear MRI reconstruction using moment-based spectral analysis," *IEEE Trans. Med. Imag.*, vol. 37, no. 2, pp. 557–567, 2017.
- [15] M. Seeger, H. Nickisch, R. Pohmann, and B. Schölkopf, "Optimization of k -space trajectories for compressed sensing by bayesian experimental design," *Magn. Reson. Med.*, vol. 63, no. 1, pp. 116–126, 2010.
- [16] B. Gözcü, R. K. Mahabadi, Y.-H. Li, E. Ilıcak, T. Çukur, J. Scarlett, and V. Cevher, "Learning-based compressive MRI," *IEEE Trans. Med. Imag.*, vol. 37, no. 6, pp. 1394–1406, 2018.
- [17] B. Zhao, J. P. Haldar, C. Liao, D. Ma, Y. Jiang, M. A. Griswold, K. Setsompop, and L. L. Wald, "Optimal experiment design for magnetic resonance fingerprinting: Cramer-rao bound meets spin dynamics," *IEEE Trans. Med. Imag.*, vol. 38, no. 3, pp. 844–861, 2018.
- [18] F. Sherry, M. Benning, J. C. De los Reyes, M. J. Graves, G. Maierhofer, G. Williams, C.-B. Schönlieb, and M. J. Ehrhardt, "Learning the sampling pattern for mri," *IEEE Trans. Med. Imag.*, 2020.
- [19] K. H. Jin, M. Unser, and K. M. Yi, "Self-supervised deep active accelerated MRI," *arXiv preprint arXiv:1901.04547*, 2019.
- [20] M. Mardani, G. Mateos, and G. B. Giannakis, "Subspace learning and imputation for streaming big data matrices and tensors," *IEEE Trans. Signal Process.*, vol. 63, no. 10, pp. 2663–2677, 2015.
- [21] A. Krishnamurthy and A. Singh, "Low-rank matrix and tensor completion via adaptive sampling," in *Proc. Adv. Neural Inf. Process. Syst.*, 2013, pp. 836–844.
- [22] X.-Y. Liu, S. Aeron, V. Aggarwal, X. Wang, and M.-Y. Wu, "Adaptive sampling of rf fingerprints for fine-grained indoor localization," *IEEE Trans. Mobile Comput.*, vol. 15, no. 10, pp. 2411–2423, 2015.
- [23] L. Deng, H. Zheng, X.-Y. Liu, X. Feng, and Z. D. Chen, "Network latency estimation with leverage sampling for personal devices: An adaptive tensor completion approach," *IEEE/ACM Trans. Netw.*, 2020.
- [24] C. J. Hillar and L.-H. Lim, "Most tensor problems are np-hard," *J. ACM*, vol. 60, no. 6, pp. 1–39, 2013.
- [25] J. Liu, P. Musialski, P. Wonka, and J. Ye, "Tensor completion for estimating missing values in visual data," *IEEE Trans. Pattern Anal. Mach. Intell.*, vol. 35, no. 1, pp. 208–220, 2012.
- [26] S. F. Roohi, D. Zonoobi, A. A. Kassim, and J. L. Jaremko, "Multi-dimensional low rank plus sparse decomposition for reconstruction of under-sampled dynamic MRI," *Pattern Recognit.*, vol. 63, pp. 667–679, 2017.
- [27] H. S. Seung, M. Opper, and H. Sompolinsky, "Query by committee," in *Proc. Annu. Workshop Comput. Learn. Theory*, 1992, pp. 287–294.
- [28] E. J. Candès and B. Recht, "Exact matrix completion via convex optimization," *Found. Comput. Math.*, vol. 9, no. 6, p. 717, 2009.
- [29] A. Eftekhari, M. B. Wakin, and R. A. Ward, "Mc2: A two-phase algorithm for leveraged matrix completion," *Inf. Inference*, vol. 7, no. 3, pp. 581–604, 2018.
- [30] A. Andreopoulos and J. K. Tsotsos, "Efficient and generalizable statistical models of shape and appearance for analysis of cardiac MRI," *Med. Image Anal.*, vol. 12, no. 3, pp. 335–357, 2008.